Measurement of the energy penetration depth into solid targets irradiated by ultrashort laser pulses

M. Fraenkel,[1] A. Zigler,[1] Z. Henis,[2] S. Eliezer,[2] and N. E. Andreev[3]
[1]*Racah Institute of Physics, Hebrew University, Jerusalem, Israel*
[2]*Plasma Physics Department, Soreq NRC, Yavne 81800, Israel*
[3]*High Energy Density Research Center, Joint Institute for High Temperatures, Russian Academy of Sciences, ul. Izhorskaya 13/19, Moscow, 127412 Russia*
(Received 12 August 1999)

The energy penetration depth of a short (100 fs) Ti-sapphire laser pulse (0.8 μm) of intensity 3×10^{16} W/cm^2, in solid density materials has been measured. High-Z (BaF_2) and low-Z (MgF_2) solid layers targets were used. The penetration depth was determined from the measurement of the x-ray emission spectra, as a function of the target thickness. The investigation of these spectra showed that in the low-Z case, solid density material to a depth of 50 nm was heated to a peak electron temperature of ~150 eV. For the high-Z material, the penetration depth corresponding to this temperature exceeded 100 nm. This is evidence of a larger heat penetration depth in a high-Z material in comparison to a low-Z material. A model based on electron heat conduction is used to estimate the energy penetration depth. It is suggested that the larger heat penetration in high-Z material is due to heating of the material, caused by the radiation flux, generated by the electron heat conduction.

PACS number(s): 52.70.−m

The recent development of high-power ultrashort lasers based on chirped pulse amplification (CPA) [1] has opened the opportunity to study the physics of plasma at solid density and high temperatures [2–12]. High intensity laser pulses with 100 fs duration can interact directly with supercritical density plasmas and heat solid density material to high temperatures, before significant hydrodynamic expansion takes place. During the interaction of an ultrashort laser with matter, electrons within an optical skin depth of the surface directly absorb energy from the laser. The generated hot electrons subsequently ionize much cooler atoms in the skin layer and generate solid density plasma, which can emit intense, ultrafast x-ray pulses. These x-rays have potential applications, such as in the development of x-ray lasers, in advanced fusion schemes, for microscopy of biological objects or short time diagnostics of laser plasma. The yield and duration of these short x-ray pulses depend upon the interplay of a number of effects: absorption, heating, ionization, recombination and transport. Therefore the study of the energy transport mechanisms in the plasma is very important for understanding the dynamics of ultrashort x-ray generation.

The energy transport in near solid density plasmas is reported in previous works. Zigler *et al.* [6] measured the energy penetration of a 600 fs, 248 nm, 3×10^{16} W/cm^2 laser in low-Z materials, such as SiO_2 and MgF_2. The generation of a supersonic ionization front in solid density fused quartz plasma, irradiated by a 100 fs, 5×10^{14} W/cm^2 laser pulse was reported by Vu *et al.* [10]. A radiation driven ionization wave, generated into fused silica by a 2 ps, 10^{17} W/cm^2 laser pulse, was measured by Ditmire *et al.* [11]. Measurements of x-ray emission and thermal transport in near-solid-density plasmas heated by a 130 fs, 3×10^{17} W/cm^2 laser pulses, to peak temperatures of 370 ± 50 eV were performed by Young *et al.* [12]. A study of energy transport in fused silica targets irradiated by a 2 ps laser pulse, as a function of the laser intensity, wavelength and target angle, was reported by Gumbrell *et al.* [13].

In this paper we report the experimental determination of the heat penetration depth in a high-Z material, BaF_2 and a low-Z material, MgF_2. The penetration depth was determined from the measurement of the x-ray emission spectra, as a function of the target thickness.

The laser used in this study was a Ti-sapphire laser system based on the CPA method, and was described elsewhere [14]. The energy per pulse was 20 mJ and the pulse width was 110 fs. In the experiments reported here, the laser was operated at 800 nm and with a repetition rate of 10 Hz. The prepulse/pulse extinction ratio was around 500. The materials studied here were transparent to low levels of the laser irradiance, to suppress prepulse plasma formation [15]. The laser pulse was focused on the targets by means of an $f/10$ lens. The peak laser intensity achieved on target was $(3\pm1)\times10^{16}$ W/cm^2. The target was placed in a vacuum chamber, evacuated to 10^{-5} Torr. A schematic description of the experimental setup is shown in Fig. 1. The targets con-

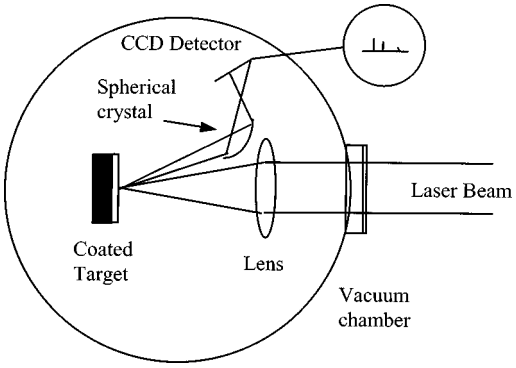

FIG. 1. Schematic description of the experimental setup.

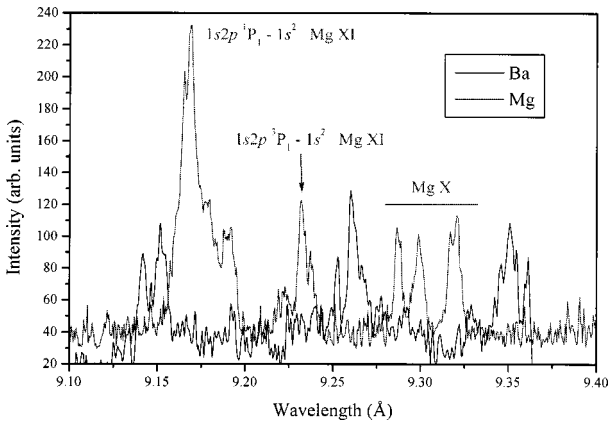

FIG. 2. Spectra of Ba and Mg in the spectral range (9.1–9.4) Å measured using bare targets.

sisted of two layers, MgF_2 substrate coated with BaF_2 of known thickness, for the experiments aimed to determine the energy penetration depth in BaF_2. The penetration depth in MgF_2 was measured using BaF_2 substrate coated with MgF_2 of known thickness. The x rays emitted from the plasma created on the targets were collected using spherically bent mica crystal spectrometers [14] and recorded with a CCD camera with a spectral sensitivity in the x-ray region. The mica crystal technique has a very high spectral resolution, $\lambda/\Delta\lambda \sim 10^4$, which enables better insight into unresolved spectral features.

The spectral range measured in the experiments was (9.1–9.4) Å. This spectral region includes mainly the $3d$-$6f$ transitions of Cu-like and Zn-like barium, the $3d$-$7f$ transition of Ga-like barium, and He-like and Li-like satellite lines in Mg. The high spectral resolution used in the experiments allowed the detection of these lines. The spectra of Ba and Mg in the above spectral range are shown in Fig. 2. These spectra were measured using bare targets of BaF_2 and MgF_2, respectively.

The spectra in the range (9.1–9.4) Å, emitted from a two-layer target, consisting of BaF_2 substrate coated with 100, 75, and 50 nm of MgF_2 are shown in Fig. 3. In these experiments, the laser irradiated the MgF_2 coatings and then the

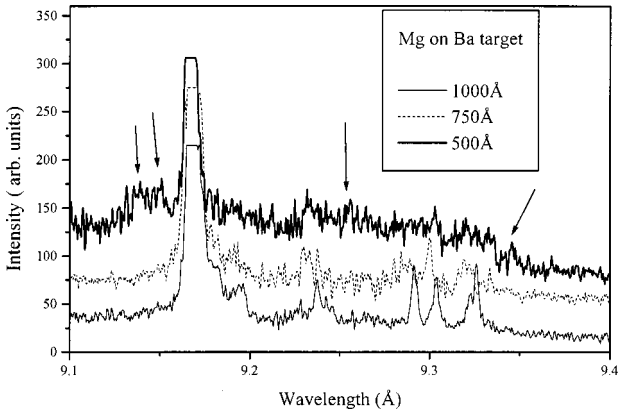

FIG. 3. The x-ray emission in the range (9.1–9.4) Å from two layer targets, consisting of a BaF_2 substrate and a 50, 75, and 100 nm MgF_2 coating. The arrows indicate Cu-like Ba lines, emitted from the target with 50 nm coating.

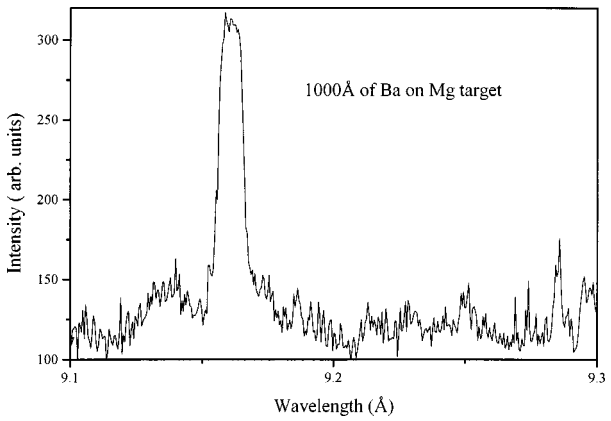

FIG. 4. The x-ray emission in the range (9.1–9.4) Å from a two layer targets, consisting of a MF_2 substrate and a 100 nm BaF_2 coating. The spectrum contains both Cu-like Ba lines and He-like Mg lines.

energy was transported into the bulk region of the target. Several $3d$-$7f$ Cu-like Ba lines (designated by the arrows) are seen in the spectrum corresponding to the 50 nm MgF_2 coating. The electron temperature required for the emission of the above lines is of the order of 150 eV [14]. No Ba lines were detected in the experiments performed with the targets with 75 and 100 nm MgF_2 coatings. These results indicate that solid density MgF_2 was heated to an electron temperature of 150 eV to a depth of 50 nm.

The spectrum in the range (9.1–9.4) Å, emitted from a two-layer target, consisting of MgF_2 substrate coated with 100 nm BaF_2 is shown in Fig. 4. It is seen that this spectrum contains both Cu-like Ba lines and He-like Mg lines. This indicates that the BaF_2 was heated to a temperature of 150 eV, to a depth of 100 nm.

The above experiments reveal that the energy penetration depth is larger for the high-Z material Ba than for the low-Z material Mg.

In order to explain the experimental results an estimation of the electron temperature into the target, as a function of depth was made. When the laser pulse interacts with a solid, a high temperature and solid density plasma layer is quickly produced at the target surface by the leading edge of the laser pulse. This plasma layer prevents the remainder of the laser pulse from penetrating into the colder underlying bulk region behind the surface. The remainder of the laser pulse deposits its energy to the plasma electrons at the surface. The energy absorbed at the surface is transported into the bulk region via electron thermal conduction supersonically, until plasma expansion becomes important. The plasma density and temperature, the thickness of the skin layer, and the absorption coefficient of the laser energy are interrelated quantities, which vary with time. The calculation of the electron temperature must include the laser energy absorption, ionization by the electromagnetic field and by electron impact, the exact electron energy distribution, the level populations, electron-ion energy relaxation, the x-ray emission spectrum, the heating of the produced plasma, hydrodynamic expansion, and shock wave generation. Complex simulations, such as LASNEX [16] and more recent short pulse codes [17–19] take into account the main pieces of the complex interaction physics. However previous experiments [3,11] showed that

analytic scaling laws might be used to predict the response of the plasma as a function of the laser parameters.

An important parameter for estimating the electron temperature is the laser energy absorption fraction. Assuming first that the absorption fraction is constant in time, the electron temperature and the heat penetration depth can be found by equating the incident heating flux to the classical thermal conduction [3]. For the laser intensities considered here, the depth of the skin layer l_s is usually small ($l_s \approx 10$ nm). The depth of the energy penetration is larger than the depth of the skin layer and so the heat conduction is of classical diffusion nature. Therefore the target heating can be modeled by the propagation of a thermal wave in semi-infinite plasma with a given flux at the boundary:

$$\frac{3}{2} n_e k_B \frac{\partial T}{\partial t} = -\frac{\partial q}{\partial x}, \quad q = -\kappa(T) \frac{\partial T}{\partial x}, \tag{1}$$

n_e is the electron density and the electron thermal conductivity is estimated by the Spitzer-Harm conductivity

$$\kappa = \frac{4 k_B (k_B T)^{5/2}}{m_e^{1/2} (Z+1) e^4 \ln \Lambda}. \tag{2}$$

m_e is the electron mass, e is the electron charge, $k_B T$ is the electron thermal energy, Z is the average charge of the plasma, and $\ln \Lambda$ is the Coulomb logarithm, assumed constant ($\ln \Lambda = 3$) in the calculation here. The boundary conditions for the heat conduction equation (1) is

$$q(0,t) = AI, \quad q(\infty, t) \to 0. \tag{3}$$

I is the laser intensity and A is the absorption fraction. It is assumed in Eq. (1) that the plasma is formed instantaneously and the energy required for ionization is neglected. In the following estimation of the temperature it is also assumed that there are no hydrodynamic effects and the electron density is constant. The plasma specific heat is given by the ideal gas law. The time and space dependence of the peak electron temperature is given by the similarity solution of Eq. (1). For times smaller than t_1, the laser pulse duration, and assuming a flat top time dependence for the laser pulse, the peak temperature is

$$T_a[\mathrm{eV}] = 92 \left(\frac{I_{\mathrm{abs}}}{10^{16}\ \mathrm{w/cm^2}} \right)^{2/7} \left(\frac{x}{\mathrm{nm}} \right)^{2/7} Z^{2/7}. \tag{4}$$

The absorbed laser irradiance is $I_{\mathrm{abs}} = IA$, $n_e = Z n_i$ is the ion density and x is the depth into the target, corresponding to the peak temperature T. The electron temperature at times larger than the pulse duration are given by [3,20]

$$T_b[\mathrm{eV}] = 4.2 \times 10^5 \frac{[F/(10^{16}\ \mathrm{W/cm^2}\ 100\ \mathrm{fs})]}{Z(n_i/6\times 10^{22})(x/\mathrm{nm})}. \tag{5}$$

$F = I_{\mathrm{abs}} t_1$ is the fluence.

Next we consider a time dependent absorption coefficient. The laser energy in the supercritical plasma is absorbed due to electron collisions in the skin layer, or due to collisionless mechanisms, depending on the laser intensity and relationship between the electron mean free path, skin depth, laser frequency, collision frequency, and electron thermal velocity [21–23]. In the case of relatively low laser intensities ($I \leqslant 10^{16}$ W/cm^2) the plasma heating occurs due to collisions. Two absorption mechanisms exist in this regime, the normal skin effect and the high frequency skin effect. For laser intensities in excess of several 10^{16} W/cm^2 the role of collisions decreases. Collisionless mechanisms of absorption, such as the anomalous skin effect and the sheath inverse bremsstrahlung [21–23], become dominant. In the experimental conditions here the laser energy absorption occurs in the regime of the normal skin effect (NSE). In this case the absorption coefficient and the depth of the skin layer are given by

$$A = \frac{2 \omega_0 l_s}{c}. \tag{6}$$

ω_0 is the laser frequency, and the depth of the skin layer for the normal skin effect is

$$l_s = \frac{c}{\omega_{pe}} \left(\frac{2 \nu_{\mathrm{eff}}}{\omega_0} \right)^{1/2}. \tag{7}$$

c is the velocity of light, ω_{pe} is the plasma frequency, and the classical expressions for the collision frequency is

$$\nu_{\mathrm{eff}} = \frac{\frac{4}{3} (2\pi)^{0.5} e^4 \ln \Lambda Z n_e}{m_e (k_B T)^{3/2}}. \tag{8}$$

A self-similar solution of Eq. (1) can be found [21], using Eqs. (6)–(8). The peak temperature and the coefficient of absorption A as a function of time are given by

$$T_c[\mathrm{eV}] = 6 I Z^{6/17} \left(\frac{I}{10^{16}\ \mathrm{W/cm^2}} \right)^{4/17} \left(\frac{\lambda}{\mu\mathrm{m}} \right)^{-2/17} \left(\frac{x}{\mathrm{nm}} \right)^{4/17} \times \left(\frac{n_i}{6\times 10^{22}\ \mathrm{cm^{-3}}} \right)^{-11/18}, \tag{9}$$

$$A = 0.039 Z^{-3/8} \left(\frac{I}{10^{16}\ \mathrm{W/cm^2}} \right)^{-1/4} \left(\frac{\lambda}{\mu\mathrm{m}} \right)^{-3/8} \left(\frac{t}{100\ \mathrm{fs}} \right)^{-1/8} \times \left(\frac{n_i}{6\times 10^{22}\ \mathrm{cm^{-3}}} \right)^{-7/24}. \tag{10}$$

The laser absorption fraction was not measured in the experiments here. Price *et al.* [24], measured the absorption coefficient for a variety of materials at laser intensities in the range 10^{13}–10^{18} W/cm^2. Their results [24] showed that at laser intensity $(3 \pm 1) \times 10^{16}$ W/cm^2, the absorption coefficient was in the range (8–15)%, depending on the material and the intensity. Higher values of the absorption fraction were reported as well. An absorption in the 10–30 % range is indicated in Refs. [2,3,6] for similar laser intensities. A coefficient of absorption of 40% was reported in Refs. [11,13]. Figure 5 shows the absorption coefficient during the laser pulse in the regime of the normal skin effect, calculated using Eq. (13), for values of the laser intensity in the range 2×10^{16} to 4×10^{16} W/cm^2. It is seen that that the absorption coefficient given by the scaling laws characteristic to the normal skin effect is by more than 30% higher

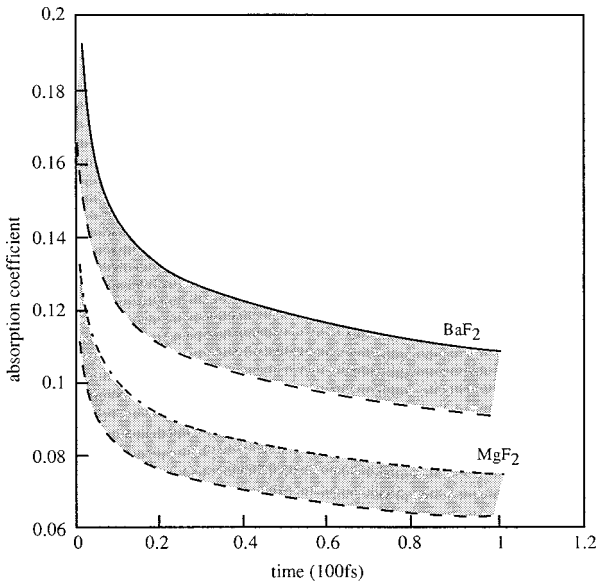

FIG. 5. The absorption coefficient as a function of time, for three values of the laser intensities in BaF_2 and MgF_2: in the range 2×10^{16} to 4×10^{16} W/cm^2.

in BaF_2 than in MgF_2. These values of the absorption coefficient are in agreement with those measured in Ref. [24], but lower than reported in Refs. [2,3,6,11,13].

In the experiments reported here the peak electron temperature was determined from the measured x-ray spectrum, for different depths of the target. From the measured spectra, it was concluded that the degree of ionization was 29 in barium, 10 in magnesium, and 9 in fluorine. The peak electron temperature as a function of the depth into the target, calculated by Eqs. (4), (5), and (9) is shown in Fig. 6. The electron temperature displayed in this figure, for the case of constant absorption, was calculated using the value of the absorption coefficient given by the normal skin effect, averaged over the laser pulse ($A=0.11$ in BaF_2 and $A=0.08$ in MgF_2). It is seen that in BaF_2 the depth of penetration of the peak temperature during the laser pulse, calculated assuming constant absorption coefficient and NSE, is about 70 nm. The peak temperature at a depth of 100 nm is about 100 eV, smaller than the temperature deduced from the spectra measured in the experiments. In MgF_2 the penetration depth of the peak temperature during the laser pulse, is about 110 nm, according to the NSE and about 60 nm, assuming a constant coefficient of absorption. The peak temperature at the end of the laser pulse is about 300 eV in the case of constant absorption. The peak temperature at a depth of 100 nm in the case of constant absorption is about 80 eV. Therefore it seems that the experimental results obtained with the MgF_2 targets are in agreement with the model describing the material heating by electron heat conduction, assuming constant absorption. The NSE does not fit to the experiments in MgF_2, since in predicts a much higher peak temperature at a depth of 100 nm.

As seen in Fig. 6, the peak temperature obtained in BaF_2, at a depth of 100 nm, is smaller than measured in the experiments. It is suggested that the heating of the material to the higher temperature measured in the experiments is caused by the radiation, generated by the electron heat conduction. The radiation may also be estimated using analytic scaling laws.

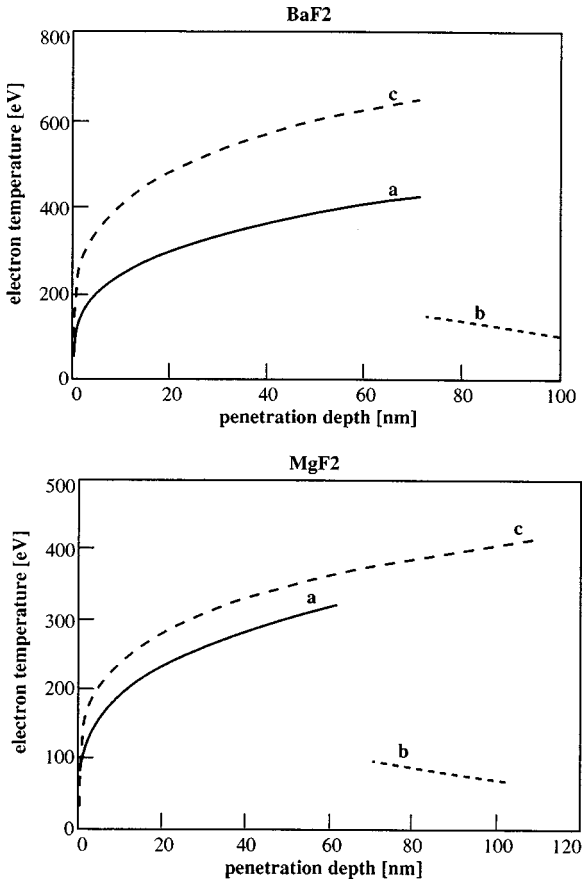

FIG. 6. The electron temperature in BaF_2 and MgF_2, as a function of the depth into the target given by the normal skin effect and assuming a constant coefficient of absorption.

As seen in Fig. 6, the heat penetration depth on the 100 fs time scale, i.e., the scale length L, is about 60 nm. The radiation Planck mean free path l is much larger than this scale length. In other words, the radiation region is optically thin and the system radiates as a diluted black body [3], with a power:

$$P=S\sigma T^4\frac{L}{l}, \tag{11}$$

S is the radiating area and σ is the Stephan-Bolzmann constant. The radiation Planck mean free path was calculated using a power law function of temperature and density $l=l_0\rho^sT^r$. The values of l_0, r, and s were calculated in Ref. [25] and are given in Table I. The maximum x-ray flux (at the end of the laser pulse) at the laser intensity 3×10^{16} W/cm^2 was 576 MW in BaF_2 and 58 MW in MgF_2. We mention that the radiation output was measured in the experiments as well, and it was found that it was by an order of

TABLE I. Parameters used in the calculation of the Planck mean free path $l=l_0\rho^sT^r$ taken from Ref. [25]. The temperature T is in keV.

	l_0	s	r
Barium	3.08×10^{-3}	-1.244	1.644
Magnesium	0.029	-1.483	2.415

magnitude higher in BaF_2 than in MgF_2. Since the material is optically thin, this x-ray flux propagates at a speed of the order of the light velocity, ahead of the heat wave generated by the electron heat conduction. A crude estimation of the temperature of the material due to the x-ray heating is given by

$$\Delta T = \frac{P}{mc_v}. \tag{12}$$

m is the mass heated by the above radiation flux, a 400 Å wide layer of BaF_2, and c_v is the specific heat. The x-ray mean free path in cold BaF_2 is $l_c \sim 0.3\,\mu$m. We consider two extreme values for the specific heat of cold BaF_2, the value for cold material, 4.1×10^6 erg/g deg, and the value for plasma, described by an ideal gas, 3.5×10^7 erg/g deg. From Eq. (5), we obtain a temperature of about 40 eV, using the specific heat of plasma and a temperature of about 350 eV for the specific heat of cold materials. Therefore the heating of the material by radiation might explain the temperature of about 150 eV, obtained from the experiments. Due to the lower conversion efficiency to x-ray in MgF_2, and a larger radiation mean free path in the cold material, the above heating generated by the radiation flux is negligible for MgF_2.

In conclusion, we have presented experimental evidence of a larger energy penetration depth of an ultrashort high intensity laser in a high-Z material, in comparison to a low-Z material. This result was obtained from spectral studies of layered BaF_2/MgF_2 targets, irradiated by a 100 fs, 0.8 μm laser, with an intensity $\sim 3\times10^{16}$ W/cm^2. An estimate of the electron temperature, based on electron conductivity and radiation preheating of the cold material, compare quite favorably with the experiments. The measured penetration depths do not follow the NSE scaling laws.

[1] D. Strickland and G. Mourou, Opt. Commun. **56**, 219 (1985).
[2] M. M. Murnane, H. C. Kapteyn, and R. W. Falcone, Phys. Rev. Lett. **62**, 155 (1989).
[3] M. D. Rosen (unpublished).
[4] H. M. Milchberg, I. Lyubomirsky, and C. G. Durfee III, Phys. Rev. Lett. **67**, 2654 (1991).
[5] R. M. More, Z. Zinamon, K. H. Warren, R. Falcone, and M. Murnane, J. Phys. (Paris), Colloq. **61**, C7-43 (1988).
[6] A. Zigler, P. G. Burkhalter, D. J. Nagel, M. D. Rosen, K. Boyer, G. Gibson, T. S. Luk, A. McPherson, and C. K. Rhodes, Appl. Phys. Lett. **59**, 534 (1991).
[7] A. Zigler, P. G. Burkhalter, D. J. Nagel, K. Boyer, T. S. Luk, A. McPherson, J. C. Solem, and C. K. Rhodes, Appl. Phys. Lett. **59**, 777 (1991).
[8] M. M. Murnane, H. C. Kapteyn, M. D. Rosen, and R. W. Falcone, Science **251**, 531 (1991).
[9] K. Nazir, S. J. Rose, A. Djaoui, G. J. Tallents, M. G. Holden, P. A. Norrey, P. Fews, J. Zhang, and F. Failles, Appl. Phys. Lett. **69**, 3686 (1996).
[10] B. T. V. Vu O. L. Landen, and A. Szoke, Phys. Plasmas **2**, 476 (1995).
[11] T. Ditmire, E. T. Gumbrell, R. A. Smith, L. Mountford, and M. H. R. Hutchinson, Phys. Rev. Lett. **77**, 498 (1996).
[12] B. K. F. Young, B. G. Wilson, D. F. Price, and R. E. Stewart, Phys. Rev. E **58**, 4929 (1998).
[13] E. T. Gumbrell, R. A. Smith, T. Ditmire, A. Djaoui, S. J. Rose, and M. H. R. Hutchinson, Phys. Plasmas **5**, 3714 (1998).
[14] R. Doron, E. Behar, M. Fraenkel, P. Mandelbaum, A. Zigler, J. L. Schwob, A. Ya. Faenov, and T. A. Pikuz, Phys. Rev. A **58**, 1859 (1998).
[15] A. Zigler, P. G. Burkhalter, D. J. Nagel, M. D. Rosen, K. Boyer, T. S. Luk, A. Mc. Pherson, and C. K. Rhodes, Opt. Lett. **16**, 1261 (1991).
[16] G. B. Zimmerman and W. L. Kruer, Comments Plasma Phys. Control. Fusion **2**, 51 (1995).
[17] A. Ng, P. Cellier, A. Forsman, R. M. More, Y. T. Lee, F. Perrot, M. W. C. Dharma-wardena, and G. A. Rinker, Phys. Rev. Lett. **72**, 3351 (1994).
[18] J. Davis, R. Clark, and J. Giuliani, Laser Part. Beams **13**, 3 (1995).
[19] N. E. Andreev, V. V. Kostin, and M. E. Veisman, Phys. Scr. **58**, 486 (1998).
[20] Ya. B. Zel'dovich and Yu. P. Raizer, *Physics of Shock Waves and High-Temperature Hydrodynamic Phenomena* (Academic Press, New York, 1967), Vol. II, Chap. 10.
[21] W. Rozmus and V. T. Tikhonchuk, Phys. Rev. A **42**, 7401 (1990).
[22] E. G. Gamaly, Laser Part. Beams **12**, 185 (1994).
[23] W. Rozmus, V. T. Tikhonchuk, and R. Cauble, Phys. Plasmas **3**, 360 (1996).
[24] D. F. Price, R. M. More, R. S. Walling, G. Guethlein, R. L. Shepherd, R. E. Stewart, and W. E. White, Phys. Rev. Lett. **75**, 252 (1995).
[25] G. D. Tsakiris and K. Eidman, J. Quant. Spectrosc. Radiat. Transf. **38**, 353 (1987).